CrystEngComm

HIGHLIGHT

View Article Online
View Journal | View Issue

Check for updates

Cite this: *CrystEngComm*, 2024, **26**, 4751

Organic charge transfer complex towards functional optical materials

Kalyan Jyoti Kalita, Rakhi Arikkottira M and Ratheesh K. Vijayaraghavan *

Received 13th July 2024,
Accepted 6th August 2024

DOI: 10.1039/d4ce00701h

rsc.li/crystengcomm

This year marks the 50th anniversary of a significant milestone in organic optoelectronics, *i.e.*, the first account of metallic-like conductivity in an entirely organic material, tetrathiafulvalene–tetracyanoquinodimethane (TTF–TCNQ). Since the discovery of this prototypical TTF–TCNQ charge-transfer (CT) pair, countless studies, ranging from various aspects, have been done on this fascinating TTF–TCNQ and related CT complexes. More recently, the CT complex-based approach has emerged as an elegant way of designing various next-generation functional organic materials, *viz.* room temperature phosphorescent (RTP), thermally activated delayed fluorescent (TADF), near infra infrared (NIR) emissive, organic spin-systems, *etc.* This highlight discusses how the synergy between computational screening and crystal engineering principles can be used to obtain the desired functional output and modulate the CT complex's bulk optical and electronic features. Emphasis is given to some of the recent non-covalent CT complex-based approaches to designing functional optical materials like RTP, TADF, NIR-emissive, chiral CT complex, *etc.*

Published on 13 August 2024. Downloaded on 11/19/2024 1:41:25 PM.

1. Introduction

Broadly defined, a molecular charge transfer complex is formed between two or more molecules followed by a partial or complete charge transfer that occurs from one molecular entity (donor) to another (acceptor) in their electronic ground state (Fig. 1a).[1–4] The formation of such complexes is primarily guided by the electrostatic interaction between molecules of different electron-affinity/electro-positivity and has evolved with a great interest in materials science. Organic charge transfer complexes (OCTCs) can be the basis for developing advanced materials with unique optical and electronic properties. This opens up possibilities for designing new materials with tailored functionalities, such as materials with high electrical conductivity for electronics or materials with desired optical properties.[1–10] Besides practical applications, OCTCs are of fundamental interest in chemistry and can help us better understand the nature of chemical bonding, types of molecular interactions, and charge transfer processes. They provide insights into the electronic structure and reactivity of molecules. All of the optical and electronic characteristics revolve around the CT states (Fig. 1b), which emerge from the blending of the highest occupied molecular orbital (HOMO) of the donor and the lowest unoccupied molecular orbital (LUMO) of the acceptor pair, as shown in Fig. 1.[1–4]

Department of Chemical Sciences, Indian Institute of Science Education and Research Kolkata, Mohanpur, Nadia, West Bengal, India-741246.
E-mail: ratheesh@iiserkol.ac.in.in

Since identifying the prototypical combination of TTF–TCNQ as a CT pair,[1,2] extensive research has been conducted on this intriguing TTF–TCNQ duo and similar CT complexes, exploring many angles.[3–10] Recently, there has been a growing recognition of the CT complex-based strategy as an elegant method for developing various advanced organic optical materials with functionalities such as phosphorescence, thermally activated delayed fluorescence (TADF), and more.[3–10] This comprehensive highlight delves into the functional optical attributes of CT co-crystals, shedding light on their significance in contemporary research, starting from the preparation methods. Organic charge transfer complexes (OCTCs) are appealing for designing optical materials due to their tunable optical properties, high extinction coefficients, versatility in material design, tailorable energy levels, solution processability and mechanical compliance. These properties enable the fabrication of efficient and customisable optical materials for various applications.[1–10]

2. Methods of preparation

Various methods have been widely used to prepare OCTCs, such as solid-state grinding, physical vapour transfer, and solution assembly, which are some of the most popular techniques.[9–14] The preparation process depends on the quality, chemical stoichiometry, and molecular packing pattern of donor–acceptor pairs in such co-crystals. A balance between the driving forces of thermodynamics and

Published on 13 August 2024. Downloaded on 11/19/2024 1:41:25 PM.

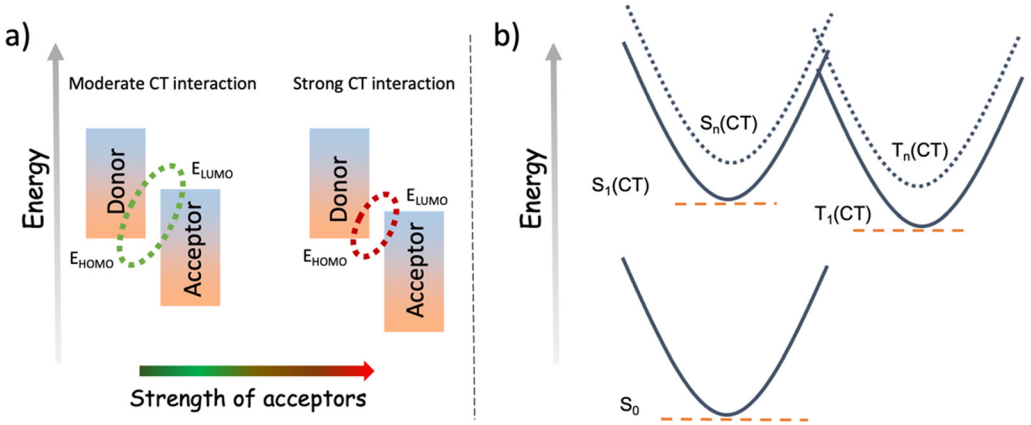

Fig. 1 a) Schematic representation of the hybridisation of the HOMO (of the donor) and LUMO (of the acceptor) in OCTC. b) Diagrammatic representation of the ground and excited CT state(s) that emerges due to the formation of the CT complex.

growth kinetics must be considered during the OCTC formation.

2(a) Solution-based method

Co-crystalising supramolecular hybrids involve liquid-phase methods like solution evaporation or standing. In general, the concentration of the donor and acceptor determines the composition and structure of the resulting co-crystals.[9] Various techniques, such as ultrasonication or magnetic stirring, can be employed to control the size of the co-crystals. Solvent choice plays a crucial role in determining the morphology and quality of the co-crystals. Solution cooling is commonly used to form supramolecular frameworks, especially when co-crystals have poor solubility at low temperatures. Usually, many micro/nano-crystals can be generated by depositing the mixed solution, with a specific mole ratio, onto substrates, followed by the evaporation of the solvent, as illustrated in Fig. 2a.

2(b) Physical vapour transport method

Physical vapour transport (PVT) involves sublimating materials in a vacuum or under the inert gas flow condition to grow OCTC

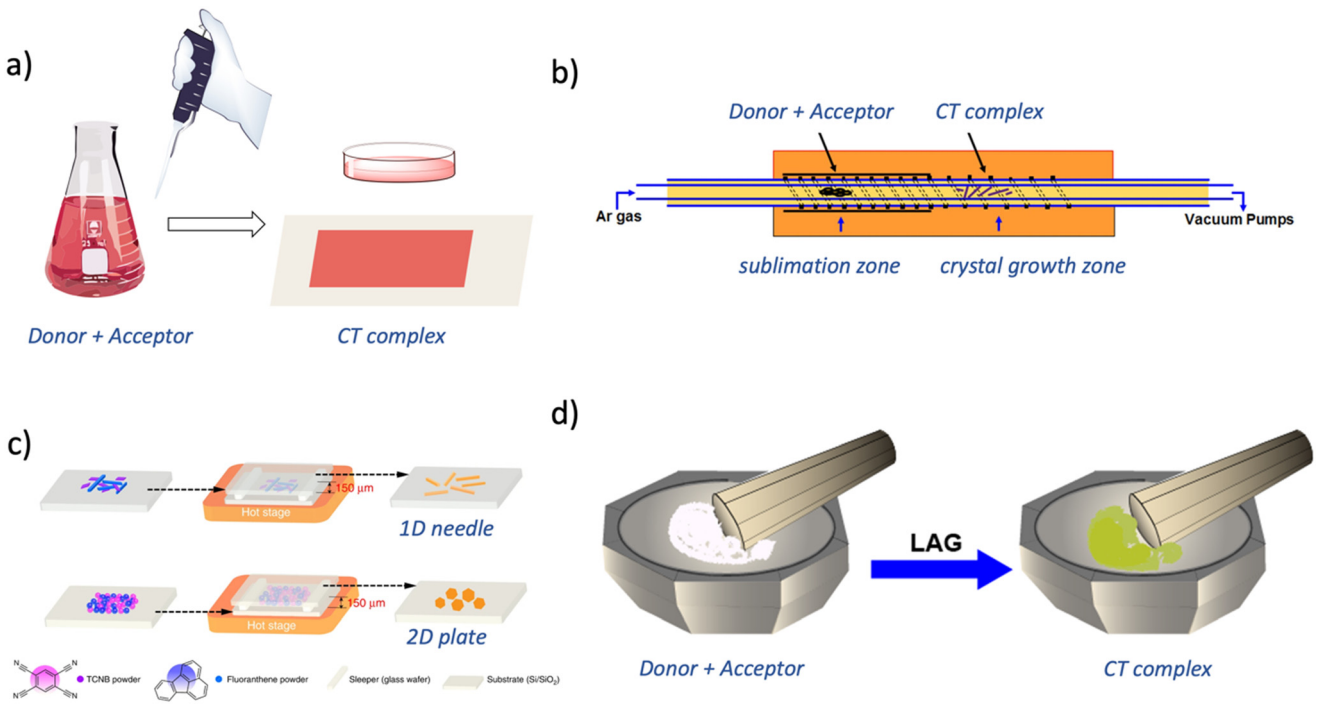

Fig. 2 Illustration of different synthesis methods: a) drop-casting; b) physical vapour transport (PVT); c) micro spacing in-air sublimation (MAS) (this figure has been adapted/reproduced from ref. 10 with permission from Springer Nature, copyright 2019); and d) mechanochemical liquid-assisted grinding (LAG).

 This journal is © The Royal Society of Chemistry 2024

Published on 13 August 2024. Downloaded on 11/19/2024 1:41:25 PM.

crystals. A quartz tube with a sealed end attached to a vacuum line must be set under a specific temperature gradient where components are co-sublimated and transported to a lower-temperature zone where the crystallisation process happens (Fig. 2b).[9] The purity of the individual components and their thermal stability uniformity in sublimation affect crystal quality and the composition ratio. PVT may yield different phases or compositions than solution processes, posing challenges for separation and applications. However, precise control of temperature and gas flow enables the separation and production of oriented polycrystalline thin films.[9]

2(c) Microscopic in-air sublimation (MAS) method

Recently, a new technique, MAS, has been developed to tackle the challenges posed by expensive vacuum systems and time-consuming processes.[10] This method enables the direct growth of organic co-crystals (including various polycyclic aromatic hydrocarbon (PAH)–acceptor complexes and pharmaceutical co-crystals bonded by hydrogen) on a substrate. These co-crystals, formed through this binary process, can take on either a needle-like 1D morphology or a plate-like 2D shape, with the specific outcome dependent on factors such as temperature and the method of mixing the initial materials (Fig. 2c). By this technique, CT co-crystals (anthracene–TCNB, pyrene–TCNB, and fluoranthene–TCNB) comprising different electron-rich PAHs (anthracene, pyrene, fluoranthene, *etc.*) with electron-deficient 1,2,4,5-tetracyanobenzene (TCNB) were grown successfully, showing enhanced luminescence due to charge transfer transitions. Morphology control was achieved by adjusting the mixing and distribution of component molecules on the bottom substrate (Fig. 2c), resulting in 1D needle-like or 2D plate-like crystals.[10]

2(d) Mechanochemical synthesis of charge transfer complex

Recently, mechanochemical approaches such as grinding, ball milling, crushing, and shearing have gained tremendous attention due to clean and green preparation methods.[11–14] Several factors, such as the material of the milling jar, frequency of vibration, nature and the quantity of liquid/solid additives used (in liquid-assisted grinding, LAG), number of balls used during milling, ball size or ball mass, milling temperature, *etc.* can influence the outcome of a mechanochemical transformation compared to solution-phase crystallisation. Fig. 2d represents the most widely used mechanochemical liquid-assisted grinding (LAG) method to prepare the CT complex. New mechanochemical techniques, such as resonance acoustic mixing (RAM), speed mixing, *etc.*, have also been developed in recent decades.[11–14]

3. CT complex: an emerging class of materials with diverse optical functionalities

Of late, OCTCs have emerged as an attractive class of optical materials.[15–24] Due to the strong electronic coupling between the donor and acceptor molecules, they exhibit relatively small energy gaps compared to individual components (Fig. 1). A small energy gap between the ground and excited states enhances the transition probability and increases the oscillator strength. A high oscillator strength indicates a high transition probability and, consequently, strong absorption or emission. The oscillator strength (f) is related to the transition dipole moment (μ) by the following equation:[25]

$$f \propto |\mu|^2$$

Moreover, the CT complex-based approach gives enough flexibility to control the bulk optoelectronic properties, enabling the design of materials with tailored electronic and optical properties for various applications such as sensors, photovoltaics, and molecular electronics. To control the bulk optical and transport properties of the CT complexes, fine-tuning the degree of the charge transfer between the D and A units is essential to achieve the best functional output. Even though CT complexes are known to show optoelectronic properties different from their components, they retain the intrinsic properties of the donor and the acceptor to some extent. For example, co-crystals based on fluorescent acceptors like TCNB and 1,4-diiodotetrafluorobenzene usually show luminescent properties. Contrary to that, the CT complex formed using strong acceptors like fullerene and F_n-TCNQ (n = 0, 1, 2, 4) mainly display transport properties in line with one component, F_nTCNQ or fullerene. A list of typical organic donor and acceptor units used for OCTC is shown in Fig. 3. Non-covalent interactions, *viz.* π–π stacking,[26] halogen and hydrogen bonding,[27,28] are the perfect toolboxes for fine-tuning the extent of charge transfer interactions. Thus, they help in achieving the desired properties from CT co-crystals. Halogen and hydrogen-bonded synthons have been observed to provide an excellent strategy to fine-tune the charge transfer interactions and thereby help achieve multifunctional CT co-crystals.[27,28] Quantifying the degree of charge transfer (DCT) in a CT complex involves various experimental and theoretical methods.[3,6,9,18,24] Here are some approaches commonly used to quantify the DCT:

UV-vis spectroscopy is one of the most commonly used experimental techniques to study the formation, electronic states and techniques to quantify DCT. The extent of charge transfer can be inferred by analysing the absorption spectra. A more significant shift in the absorption spectral maximum towards longer wavelengths (bathochromic shift) indicates a higher degree of charge transfer. Nuclear magnetic resonance (NMR) spectroscopy, especially solid-state proton (^{1}H) and carbon (^{13}C) NMR can provide valuable information about the electronic environment around the nuclei involved in the complex. Changes in chemical shifts can indicate the extent of charge transfer. Electrochemical techniques, such as cyclic voltammetry, can provide information about the redox properties of CT complexes. The difference between the redox potentials of the donor and acceptor moieties can give

Published on 13 August 2024. Downloaded on 11/19/2024 1:41:25 PM.

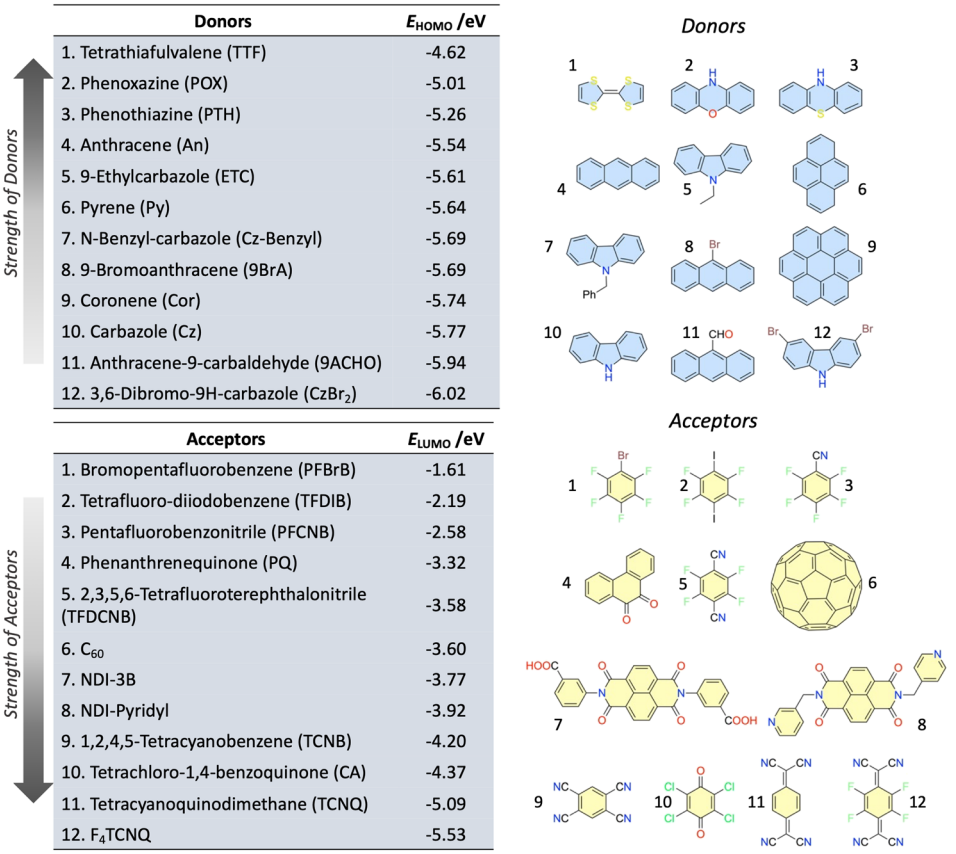

Fig. 3 Chemical structures of typical donor and acceptor molecules that are used to prepare the OCTC, along with their relative strength. HOMO and LUMO energy values are calculated at the B3LYP-GD3/def2tzvp level of theory from the optimised monomeric structure (this figure has been adapted/reproduced from ref. 29 with permission from Royal Society of Chemistry, copyright 2023).

insights into the degree of charge transfer. Fluorescence spectroscopy can be employed to study the luminescence properties of CT complexes. The extent of quenching or fluorescence enhancement upon complex formation can be correlated with the degree of charge transfer. Vibrational spectroscopic techniques have been used to quantify the degree of charge transfer, DCT (ρ), in the D–A CT complex experimentally. DCT was parametrised based on the vibrational stretching frequency. A value of ρ = 0 would indicate the completely neutral pairs with no significant intermolecular CT interactions; ρ = 1 indicates a non-interacting ion pair, while $0 < \rho < 1$ means D–A CT complexes of either mixed stack or segregated stack. Several reports used nitrile (CN) stretching frequencies of cyano-functionalised acceptors to obtain DCT (ρ) values.

$$\rho = \frac{2\Delta\nu}{\nu_0\left(1 - \frac{{\nu_1}^2}{{\nu_0}^2}\right)}$$

Here $\Delta\nu = \nu_0 - \nu_{CT}$ and ν_0, ν_1, and ν_{CT} denote the CN stretching frequencies of the acceptor in the neutral state (ρ = 0), in the anion (ρ = 1) and the CT co-crystal, respectively.

X-ray crystallography can provide detailed structural information about CT complexes, allowing for the analysis of bond lengths, bond angles, and intermolecular distances, indirectly indicating the DCT. Computational methods, such as density functional theory (DFT) or time-dependent density functional theory (TD-DFT), can provide detailed insights into the electronic structure of CT complexes. Calculating parameters like electron density redistribution, frontier molecular orbital energies, and charge transfer integrals can quantify the degree of charge transfer. A list of typical organic donor and acceptor molecules according to their electron affinity and electronegativity in monomeric state (DFT computed E_{HOMO} for donors, E_{LUMO} for acceptors) is shown in Fig. 3. Generally, a relatively strong DA pair often leads to non-luminescent OCTC.[1–4] Thus, if one would like to design a luminescent OCTC, a relatively weaker DA pair (from the list) is an ideal combination to begin with. Similarly, for RTP and TADF a donor and/or acceptor with inherently low lying triplet(s) (can be computed from monomeric state TD-DFT calculation) will be ideal. Additionally, the molecular packing motifs in the crystalline state that majorly dictates the bulk optical and electronic features of OCTC.[1–4] The molecular packing modes of OCTC can be broadly categorized as a) mixed-stack (MS) and b) segregated-stack (SS). In MS arrangement, the donor and acceptor molecular entities alternate along the stacking direction. Meanwhile, in the SS model, the donor and acceptor entities pack into separate columns of individual 8 moieties (–A–A–A– and –D–D–D–).[1–4]

 This journal is © The Royal Society of Chemistry 2024

Published on 13 August 2024. Downloaded on 11/19/2024 1:41:25 PM.

Owing to the advantage of crystal engineering, the organization of donor and acceptor pairs *via* noncovalent interactions has been a promising and convenient strategy to control the molecular packing in solids. Each technique has advantages and limitations, and employing multiple approaches can help cross-validate the results and provide a more accurate assessment.[3,6,9,18,24]

4. Cocrystal-based approach to design phosphorescent material

Organic CT co-crystals formed through non-covalent interactions such as π–π stacking,[26] hydrogen bonding, halogen bonding,[27,28] and, in addition to the electrostatic interactions, have recently garnered significant attention as two or multi-component phosphorescent materials. Many studies explore organic co-crystals exhibiting room temperature phosphorescence (RTP), elucidating the correlations between their structure, properties and corresponding electronic states.[30–34] Singh *et al.*, in a recent review, summarise some of the current advancements of organic co-crystals with room temperature phosphorescence.[30a] Similarly, Zheng *et al.*, in a recent review, highlight the advancements in enhancing RTP through supramolecular self-assembly, focusing on four main areas: self-assembly of small molecules, cocrystals,

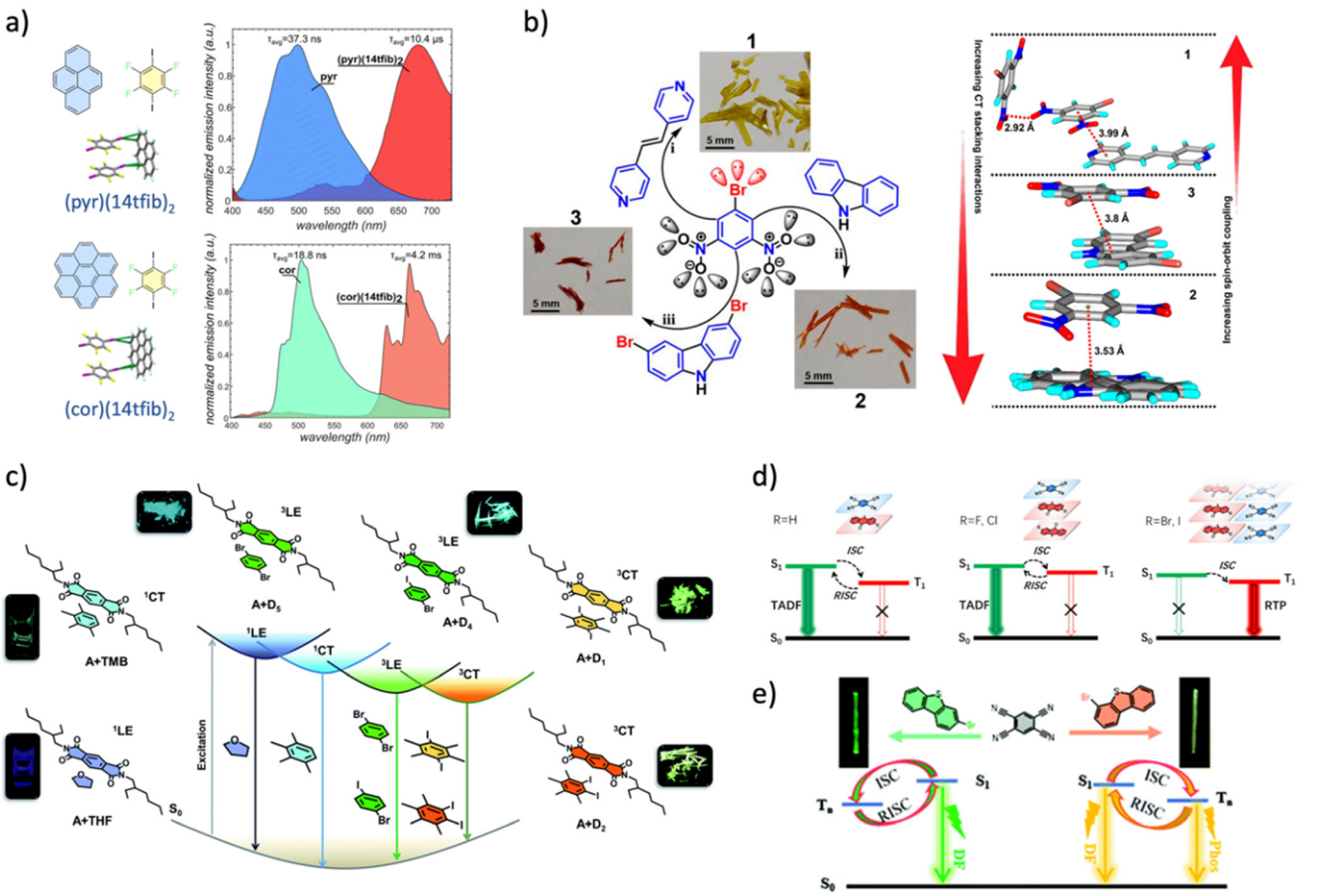

Fig. 4 a) Top: solid-state luminescence spectra for pyr (blue) and (pyr)(14tfib)$_2$; bottom: solid-state luminescence spectra for cor (green) and (cor)(14tfib)$_2$ (red). Corresponding molecular structure and simplistic 2 : 1 crystal packing are shown on the left (this figure has been adapted/reproduced from ref. 34 with permission from Royal Society of Chemistry, copyright 2023). b) Left: molecular structure and corresponding optical image of the CT co-crystals; right: the relationship between CT stacking interactions and spin–orbit coupling of the co-crystals (this figure has been adapted/reproduced from ref. 32 with permission from American Chemical Society, copyright 2021). c) Diagram illustrating the modular donor–acceptor co-assembly technique for adjusting the pyromellitic diimide phosphor's excited state manifold. PmDI (acceptor) molecular structure and tunable emission with various aromatic donors; charge-transfer (^{1}CT) and locally excited (^{1}LE) fluorescence in electron-rich aromatic solvents (*p*-xylene, mesitylene, and TMB); locally excited phosphorescence (^{3}LE) in 1-bromo-4-iodobenzene (D_4), 1-bromo-5-iodobenzene (D_5); and charge-transfer (^{3}CT) phosphorescence in 1,4-diiodo-2,3,5,6-tetramethylbenzene (D_1) and 1,2-diiodo-3,4,5,6-tetramethylbenzene (D_2). Simplified Jablonski diagram illustrating the several emission processes that can occur when an object is excited (images of ^{1}LE and ^{1}CT emission captured by a Xe lamp excitation at 340 nm and 370 nm, and ^{3}LE and ^{3}CT phosphorescent co-crystals exposed to a 365 nm UV lamp) (this figure has been adapted/reproduced from ref. 33 with permission from Royal Society of C, copyright 2022). d) Schematic of the luminescence mechanism of the TT-H, TT-F, TT-Cl, TT-Br, and TT-I co-crystals (this figure has been adapted/reproduced from ref. 35 with permission from American Chemical Society, copyright 2024). e) Representation of RTP and TADF mechanism of 3-BrTC + TCNB and 4-BrTC + TCNB CT complex (this figure has been adapted/reproduced from ref. 36 with permission from Royal Society of Chemistry, copyright 2022).

Published on 13 August 2024. Downloaded on 11/19/2024 1:41:25 PM.

macrocyclic host–guest assemblies, and multi-stage supramolecular self-assembly. The article showcases the progress made in these domains and addresses the key challenges in developing high-performance supramolecular RTP materials for practical biomedical applications.[30b]

Tomislev Friščić and co-workers recently presented a comprehensive study on halogen bonding as a reliable tool for the directional assembly of non-derivatised carbon-only aromatic systems into predictable supramolecular architectures. It aims to utilise halogen bonding as a powerful approach for designing supramolecular structures based on carbon as the molecular recognition site. The study establishes the reliable formation of supramolecular ladder-like motifs based on C–I$\cdots\pi_C$ halogen bonding across a wide range of aromatic hydrocarbons, including large polycyclic aromatic hydrocarbons (PAHs) and fullerene C_{60}. The halogen-bonded co-crystals exhibit diverse luminescence properties, including significant red and blue shifts in solid-state emission compared to the pure aromatic components. The 1 : 2 co-crystal of pyrene (py) and 1,4-diiodotetraflurobenzene (14tfib); {(pyr)(14tfib)$_2$} shows a remarkable bathochromic shift of almost 200 nm, with a maximum emission wavelength at 678 nm and a very long emission lifetime of 10.4 μs. The 1 : 2 co-crystal of coronene (cor) and 1,4-diiodotetraflurobenzene (14tfib); {(cor)(14tfib)$_2$} extends the emission into the near-infrared region beyond 750 nm and very long emission lifetime (4.2 ms) (Fig. 4a). The demonstration of the remarkable luminescence properties, including long-lived phosphorescence extending to near-infrared regions, highlights the potential of this approach in developing new phosphorescent materials.

A study by Venkatesh Gude and Kumar Biradha, demonstrates the significant role of non-covalent interactions in controlling the intersystem crossing behaviour in charge-transfer co-crystals of 3,5-dinitrobromobenzene (DNBB), providing insights into the optical behaviour of these organic materials.[32] The analysis reveals the influence of CT-stacking interactions on electronic transitions and phosphorescence behaviour, highlighting the potential of nitroaromatics in designing solid-state organic phosphorescent materials. They formed CT co-crystals using an electron-deficient molecule, 3,5-dinitro bromobenzene (DNBB), and electron-rich molecules such as 4,4′-bipyridyl ethylene (BPE), carbazole (CZ), and 3,6-dibromo carbazole (DBCZ). The co-crystals showed different stacking arrangements of donors and acceptors, influencing their optical behaviour and ISC rates. Notably, DNBB and co-crystal 1 (DNBB + BPE) exhibited phosphorescence, while 2 (DNBB + CZ) and 3 (DNBB + DBCZ) did not (Fig. 4b). Time-dependent density functional theory (TDDFT) studies and spin–orbit coupling calculations were utilised to rationalise the optical behaviour of DNBB and its co-crystals. Thus, the findings emphasise the importance of understanding molecular packing and intermolecular interactions in tailoring the properties of organic materials, contributing to the advancement of material design for various applications.[32]

In a recent report, Zhongfu An and co-workers synthesised a series of organic co-crystal phosphors by supramolecular assembly between 6-methyl-1,3,5-triazine-2,4-diamine (MTDA) and three aromatic dicarboxylic acids (isophthalic acid (IPA), terephthalic acid (TPA) and phthalic acid (PA)).[31] All reported co-crystals have exhibited strong non-covalent interactions, which can effectively suppress the non-radiative transitions of the triplet excitons and enhance the ISC process simultaneously. These co-crystals have strong afterglow, even at an elevated temperature (up to 150 °C). The organic co-crystal phosphors synthesised in the study exhibited an ultralong emission lifetime of up to 2.16 s, indicating the extended duration of phosphorescence emission. The authors hypothesised that achieving phosphorescence at high temperatures is facilitated by constructing organic co-crystal phosphors through supramolecular assembly. The stabilisation of triplet excitons at elevated temperatures plays a crucial role in maintaining phosphorescence, with the co-crystals showing remarkable stability even at temperatures as high as 150 °C. For MTDA-IPA-H_2O, the orientation of isolated water clusters and well-controlled molecular organisation within the crystal lattice enhance structural rigidity, effectively suppressing non-radiative transitions and enabling efficient room-temperature phosphorescence and unprecedented survival of high-temperature phosphorescence (HTP). Similarly, for MTDA-IPA-MeOH, the molecular packing within the co-crystals contributes to the suppression of non-radiative transitions, ultimately resulting in the efficient retention of green phosphorescence even at high temperatures, showcasing the achievement of HTP in the study. In sharp contrast, there was a linear chain of water molecules in the analogue co-crystal of melamine (MA)-IPA, so that the solvates would be easily destroyed by thermal vibration at higher temperatures (>100 °C). This innovative approach to altering the photophysical properties of co-crystals provides a new design strategy to generate organic phosphorescent materials with high-temperature tolerance, showing promise in the applications of temperature-sensitive scenarios.[31]

In another instance, Garain *et al.* reported modulation of the excited state emission properties of a straightforward pyromellitic diimide derivative, PmDI (A), upon complexation with suitable donor molecules with different electronic properties to show the selective harvesting of emission from its CT singlet and triplet states as well as locally excited (LE) states. They observed room-temperature phosphorescence *via* ^{3}CT in organic CT co-crystals using pyromellitic diimide as an acceptor and heavy atom-substituted aromatic molecules as donors. Their studies show that non-covalent complexation between donors and acceptors efficiently manipulates excited states (Fig. 4c). Leveraging PmDI's CT complexation potential and ease of accessing triplet states, they achieved ^{3}CT phosphorescence with 1,4-diiodo-2,3,5,6-tetramethylbenzene (D_1) and 1,2-diiodo-3,4,5,6-tetramethylbenzene (D_2) donors. These CT co-crystals exhibited greenish-yellow phosphorescence with quantum

 This journal is © The Royal Society of Chemistry 2024

Published on 13 August 2024. Downloaded on 11/19/2024 1:41:25 PM.

yields (46% and 43% in air and 71% and 65% under vacuum, for A + D_1 and A + D_2, respectively) and relatively high lifetimes in the order of μs (22.02 μs and 12.24 μs for A + D_1 and A + D_2, respectively) due to minimal vibrational dissipation and enhanced intersystem crossing. Moreover, the transition from ^{3}CT to ^{3}LE emission with 1-bromo-4-iodobenzene (D_4) and 1-bromo-5-iodobenzene (D_5) donors, demonstrate the versatility of through-space CT interactions in modulating excited states (Fig. 4c). This approach offers new avenues for designing efficient CT complex-based phosphorescent emitters with tunable emission and simplified synthesis.[33]

Wen *et al.* recently explored the transformation of thermally activated delayed fluorescence (TADF) to room-temperature phosphorescence (RTP) in charge-transfer co-crystals composed of the acceptor 1,2,4,5-tetracyanobenzene (TCNB) and halogen-substituted thioxanthone (TX) derivatives as donors (Fig. 4d). The co-crystals were prepared using a solvent evaporation method, where TX-R (R = H, F, Cl, Br, or I) and TCNB were mixed in and dissolved in a dichloromethane–methanol solution. The co-crystals exhibit distinct structural and photophysical properties based on the halogen substituent. As stated, the CT co-crystals exhibit a transformation from TADF emission in TX-H : TCNB (TT-H), TX-F : TCNB (TT-F), TX-Cl : TX-H (TT-Cl) to RTP emission in TX-BrT : TCNB (TT-Br), TX-I : TCNB (TT-I) as the atomic number of the halogen substituent on the TX derivative increases. The structural analysis reveals that the co-crystals show different packing arrangements, ranging from 1 : 1 alternative donor–acceptor stacking (TT-H) to 2 : 1 alternative donor–acceptor stacking (TT-F, TT-Cl) and separate stacking of donor and acceptor (TT-Br, TT-I). The transformation from TADF to RTP is attributed to the structural evolution of the TX-R aggregates in the CT complex. The different packing arrangements are influenced by the synergistic effect of electrostatic potential, steric hindrance, and intermolecular interactions. This work demonstrates the ability to regulate the excited-state properties of thioxanthone (TX) derivatives through co-crystallisation, which offers a new approach to modulating TADF and RTP in organic luminescent materials.[35]

In a similar line of thought, Liu *et al.* explore the modulation of excited-state processes in binary organic charge transfer (CT) co-crystals. Specifically, it investigates the impact of the substitution position of bromine (Br) atoms on the photophysical properties of CT co-crystals formed by dibenzothiophene (DBT) derivatives and 1,2,4,5-tetracyanobenzene (TCNB) (Fig. 4e). The researchers synthesised two types of CT co-crystal micro rods, 3-BrTC (3-bromo-dibenzothiophene + TCNB) and 4-BrTC (4-bromo-dibenzothiophene + TCNB), *via* a solution co-assembly approach. The 3-BrTC co-crystals exhibited green light emission with thermally activated delayed fluorescence (TADF), while the 4-BrTC co-crystals displayed yellow light emission with dual TADF and room-temperature phosphorescence (RTP) characteristics. The authors attributed these differences to the varying molecular packing and interactions in the two co-crystals, which were influenced by the position of the Br atom on the DBT donor. The structural analysis revealed that the 4-BrTC co-crystals had stronger halogen bonding and charge transfer interactions than the 3-BrTC co-crystals. These differences led to a smaller singlet–triplet energy gap (ΔE_{ST}) and enhanced spin–orbit coupling (SOC) in the 4-BrTC co-crystals, facilitating TADF and RTP emission pathways.[36]

Beyond two-component CT complexes, multi-component charge transfer complexes have recently gained interest. Adachi's group recently focused on creating non-deuterated co-crystals and their implications for crystal engineering to improve room-temperature phosphorescence (RTP) efficiency. The study investigates the relationship between crystal packing motifs and RTP characteristics in binary co-crystals composed of 1,4-diiodotetrafluorobenzene (DITFB) and polycyclic aromatic hydrocarbons (PAHs) like phenanthrene (Phen), chrysene (Chry), and pyrene (Pyr). The results show that binary co-crystals with σ-hole···π interactions (Phen–DITFB and Chry–DITFB) exhibit higher photoluminescence quantum yields (PLQYs) compared to the binary co-crystal with π-hole···π interaction (Pyr–DITFB). Ternary co-crystals, where some Phen sites are replaced with Pyr molecules, demonstrate RTP emission from Pyr and significantly improved PLQYs due to the suppression of non-radiative decay by changing the crystal packing motif. Additionally, they discuss the potential applications of RTP materials in anti-counterfeiting labels, sensing, and bioimaging. Various experimental techniques and calculations were used, including X-ray single crystal structure analysis, Hirshfeld surface analysis, transient PL characteristics, temperature dependence, and estimation of rate constants. The study also investigated the non-adiabatic, non-radiative decay process and the energy transfer from Phen to Pyr. Furthermore, deuterated ternary co-crystals using pyrene-d_{10} showed a higher PLQY and longer lifetime than non-deuterated co-crystals. The study provides valuable insights into crystal structure engineering to achieve efficient RTP from two or multi-component co-crystals.[37]

An appealing study led by Yuan and co-workers presents the co-crystallisation of melamine (MA) with two cyclic imide-based luminophores, succinimide (SI) and glutarimide (GI). They cultivated single crystals of MA, GI, and SI, as well as co-crystals of MA–GI and MA–SI. They characterised the photophysical properties of the crystals, including absorption, prompt and gated photoluminescence (PL) spectra, phosphorescence lifetimes (τ_p) and quantum yields (Φ_p), as well as the corresponding photophysical parameters such as intersystem crossing (ISC) and non-radiative transition rates. The co-crystals of MA–GI and MA–SI exhibited simultaneously enhanced Φ_p (up to 12.0%) and τ_p (up to 898 ms) compared to the single crystals. This was attributed to the rigidification of molecular conformations and the promotion of the ISC process by forming multiple hydrogen bonds and effectively clustering electron-rich units.

Published on 13 August 2024. Downloaded on 11/19/2024 1:41:25 PM.

Furthermore, the co-crystals showed excitation-dependent multicolour persistent RTP, with the emission maxima red-shifting by up to 100 nm for MA–GI and 90 nm for MA–SI, in contrast to the limited tunability observed in the single crystals. The structural analysis and theoretical calculations explained the enhanced persistent-RTP performance and colour tunability in the co-crystals. The co-crystals showed more diverse intermolecular interactions and emissive species, leading to efficient ISC and through-space charge transfer (TSCT) effects, which narrowed the singlet–triplet energy gaps and promoted the ISC process.[38]

5. CT complex-based approach to design TADF material

OCTC co-crystals based on a non-covalent approach have recently gained significant attention as promising TADF candidates.[29,39–43] As discussed above, forming OCTC through the spatial segregation of the orbital wave function, achieved by selectively pairing two non-covalently connected D and A molecules, offers distinct advantages over covalent systems. A simplified electronic states energy diagram arising from OCTC is represented in Fig. 4a. It is worth mentioning that the role of localised D (or A) centric triplet state(s) is (are) crucial for facilitating the intersystem crossing (ISC) or reverse intersystem crossing (RISC) as there is a change in orbital angular momentum going from CT state(s) to locally excited (LE) states(s) in accordance to El Sayed's rule (Fig. 5b).[44] El Sayed's rule states that transition between triplet (T) and singlet (S) state is prohibited in instances where the states possess identical orbital characteristics, as would occur if both were pure CT states due to the anticipated absence of spin–orbit coupling. Thus, the orbital nature of the S and T states, LE or CT, is deemed a crucial determinant of the efficiency of the ISC and RISC process. Three scenarios arise based on the relative position of the LE and CT states, as shown in Fig. 5a (right). Primarily to design an OCTC having TADF characteristics, from our understanding and previous reports on covalent systems, it is favourable if the CT and LE states are very close by, as shown in case II, so that there is sufficient orbital overlap between the CT and LE states to make the forbidden S_1 (CT) to T_1 (CT) transition favourable thereby harvesting almost ~100% excitons.[29,45,46] An ideal TADF emitter should have a) high photoluminescence quantum yield (PLQY), *i.e.* high f_{osc}, and b) high rate of RISC (k_{RISC}), *i.e.* small singlet–triplet energy offset (ΔE_{S-T}).[39] Most traditional TADF systems reduce ΔE_{S-T} at the expense of oscillator strength, f_{osc} (Fig. 4b). The conventionally followed geometric requisite of significant structural distortion between the D and A centre in covalent TADF systems to attain a low ΔE_{S-T} eventually results in low f_{osc}. Hence, achieving high PLQY in a conventional covalent-based molecular design presents an inherent challenge.[39] In

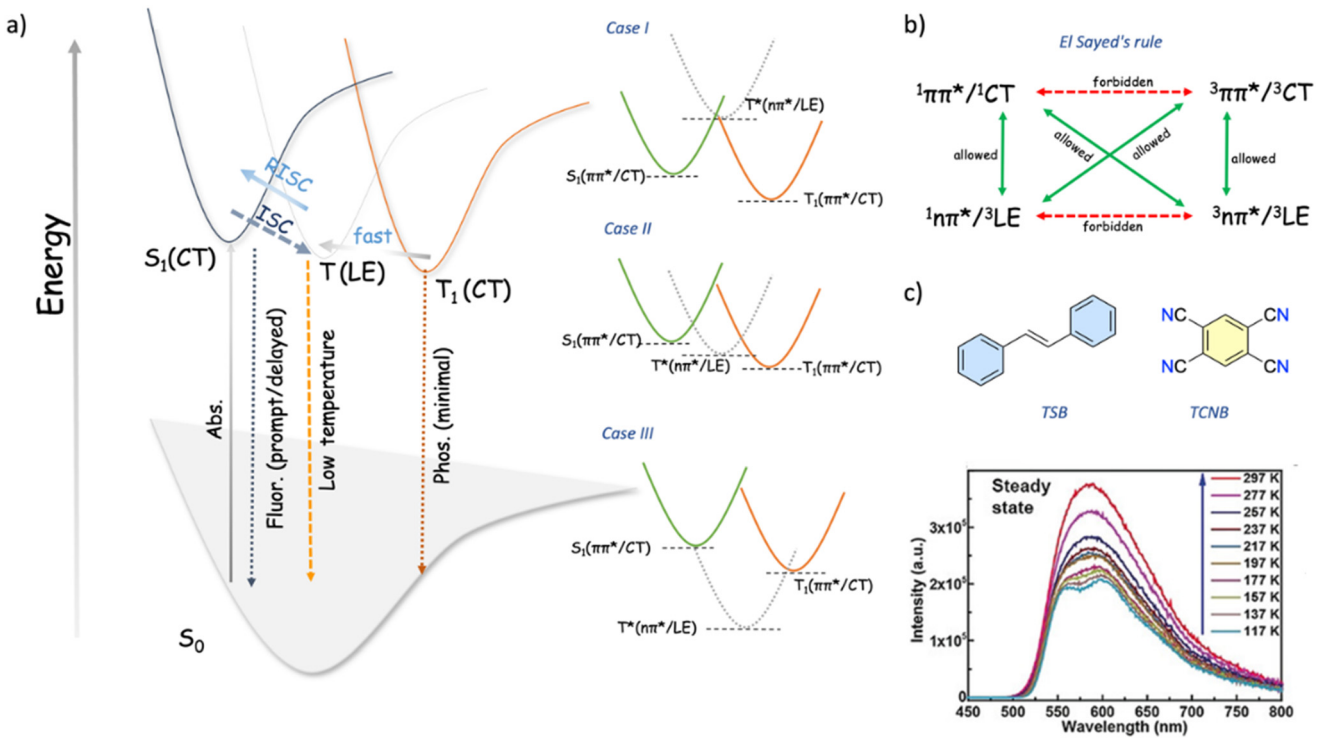

Fig. 5 a) Simplified potential energy diagram of non-covalent D and A systems to harvest triplet excitons: three possible cases of the relative position of LE and CT states are shown on the right. b) Simplified representation of El Sayed's rule. c) The molecular structure of the TSB–TCNB complex and corresponding temperature-dependent steady-state emission show a gradual increase of PL intensity with respect to temperature, the characteristic signature of the TADF emitter (this figure has been adapted/reproduced from ref. 40 with permission from Wiley, copyright 2019).

 This journal is © The Royal Society of Chemistry 2024

Published on 13 August 2024. Downloaded on 11/19/2024 1:41:25 PM.

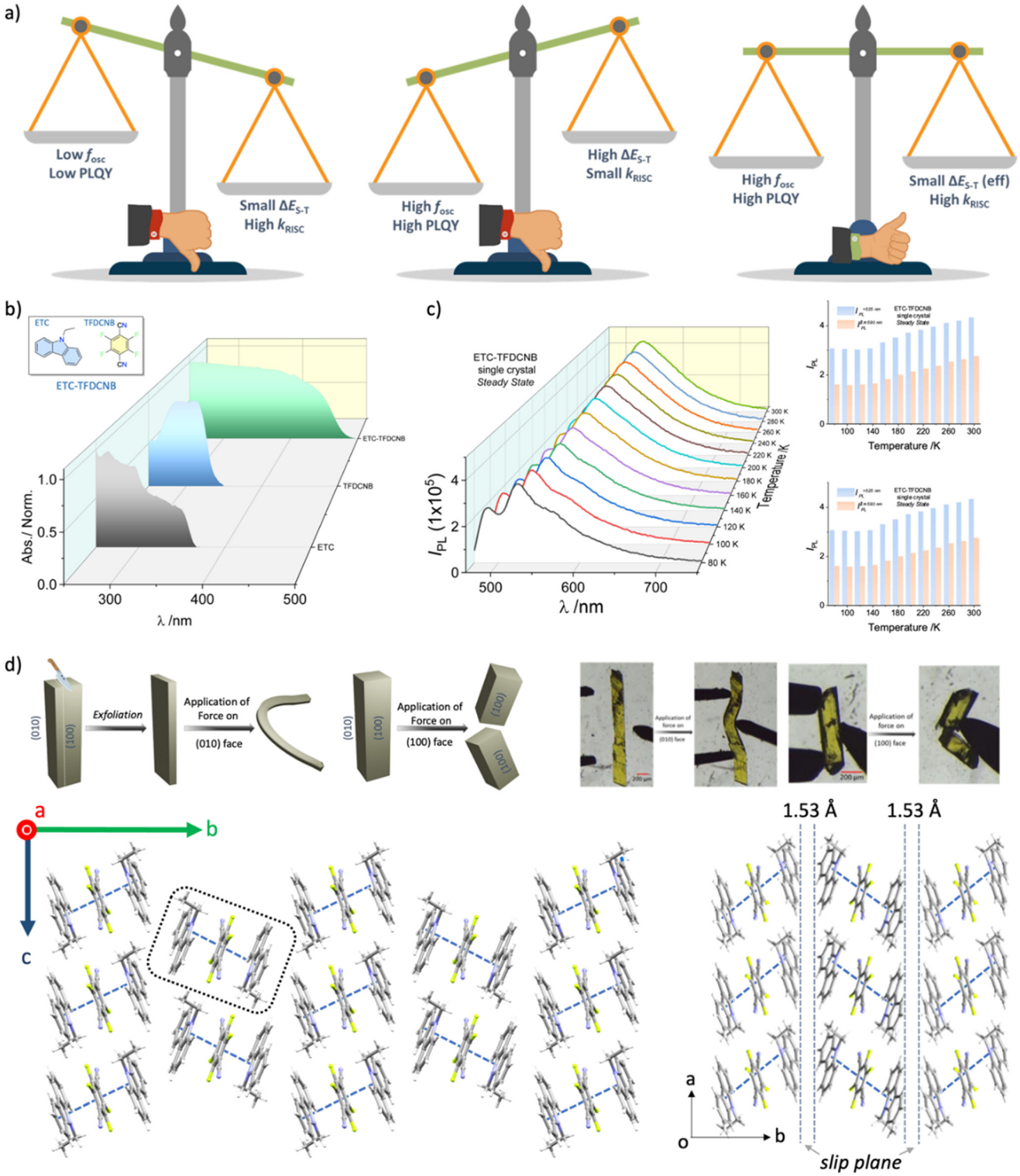

Fig. 6 a) Graphical representation of conflicting requirements of simultaneously achieving a small effective singlet–triplet energy offset and a high oscillator strength for efficient TADF emitters b) UV-visible absorption spectra (normalised at absorption maxima) of ETC, TFDCNB and the ETC–TFDCNB CT complex in the film state along with the molecular structure of ETC and TFDCNB. c) Temperature-dependent steady-state PL emission of an ETC–TFDCNB single crystal. Variation of the steady-state PL intensity and integrated area of the steady-state PL with temperature is shown along with. d) Crystal structure analysis of ETC–TFDCNB. Top: schematic representation and optical image of mechanical compliance. Bottom left: D–A–D packing of the ETC–TFDCNB co-crystal. Bottom right: the molecular packing of the ETC–TFDCNB crystal shows weak slip planes responsible for plastic deformations. This figure has been adapted/reproduced from ref. 29 with permission from Royal Society of Chemistry, copyright 2023.

Published on 13 August 2024. Downloaded on 11/19/2024 1:41:25 PM.

this context, intermolecular D and A pair-mediated TADF offer distinct advantages over the traditional intramolecular systems.[29,39–43] Tedious and sophisticated synthetic steps to obtain various C–C and C–heteroatom bonds can be eliminated by using a bimolecular pair. Additionally, compared to the poor charge balancing issue in conventional host materials in organic light-emitting (OLED) devices, the intrinsic CT bipolarity of such bimolecular systems makes this design principle more attractive.[29] The non-covalent strategy thus offers a plethora of opportunities to efficiently harvest triplet excitons as one can essentially choose a range of suitable D and A units based on their localised electronic states to regulate the electronic states of the OCTC.

Hu and coworkers have seen thermally activated delayed fluorescence (TADF) in the CT complex for the first time.[40] They successfully synthesised CT co-crystal composed of *trans*-1,2-diphenylethylene (TSB) and 1,2,4,5-tetracyanobenzene (TCNB) as donor and acceptor units, respectively (Fig. 5c). TSB–TCNB CT co-crystal (TTC) exhibits a broad emission peak at 580 nm, red-shifted compared to the individual components, indicating the formation of a CT state. The rigid co-crystal structure with strong intermolecular interactions is found to be crucial for stabilising the CT state and triplet excitons. Time-resolved photoluminescence measurements show a double-exponential characteristic of TADF-like decay with prompt and delayed lifetimes of 0.69 ms and 2.94 ms. The authors hypothesise that the intermolecular charge transfer in the co-crystal can narrow the singlet–triplet energy gap (ΔE_{ST}) and facilitate reverse intersystem crossing (RISC) to enable efficient TADF. Theoretical calculations predict a small ΔE_{ST} of 0.01–0.13 eV, facilitating RISC between the triplet and singlet states. The calculations also reveal the presence of two closely spaced triplet states (T_1 and T_2) that both contribute to the TADF process. The contribution of high-lying triplet state(s); T_2 in this particular case, in the TADF process, is becoming one of the central themes of developing highly efficient TADF systems.[40] Subsequent discussion on the nature of the high-lying triplet states will shed more light on this observation.

In a recent report, we contribute to the field by proposing a holistic, non-covalent approach for achieving efficient TADF in crystalline materials with distinct mechanical properties (Fig. 6). In the study, suitable donors and acceptors are handpicked using the crystal engineering principle and quantum chemistry calculations to realise our desired mechanical compliance and harvesting triplets *via* through-space CT interactions. Our investigation aims to circumvent the conflicting requirements (high oscillator strength and high photoluminescence quantum yield) of TADF emitters by adopting a non-covalent, crystal engineering approach. We propose that selectively choosing the donor and acceptor pair can ensure forbidden singlet–triplet transitions facilitated through a fast intersystem crossing (ISC) or reverse ISC (RISC) process, involving a donor-centric locally excited (LE) triplet state as per the classical El Sayed's rule.[44] Thus, we highlight the importance of donor-centric triplet states and propose a novel strategy involving a non-covalent design approach to balance conflicting molecular requirements for efficient TADF (Fig. 6a). As a proof-of-concept, we prepared CT complexes consisting of carbazole-derived donors *viz.* 9-ethyl carbazole (ETC) and 3,6-ditertiarybutyl carbazole (DTBC) with tetraflurodicyanobenzene (TFDCNB) as acceptor molecule using liquid-assisted grinding (Fig. 6b). The SCXRD analysis revealed a unique molecular packing in the ETC–TFDCNB complex, with a trimeric D–A–D unit that interacts in a face-to-face manner (Fig. 6d). Photophysical investigations showed a broad emission band characteristic of CT state emission, with evidence of thermally activated delayed emission (Fig. 6c). Through-space CT interactions of ETC with TFDCNB are further substantiated with the help of density functional theory (DFT) calculations. Using several control experiments, we propose a mechanism involving a sequential up-conversion process from the ^{3}CT to ^{1}CT state *via* a ^{3}LE state, enabled by the donor-centric triplet state. The presence of the donor-centric ^{3}LE state, sandwiched between the ^{1}CT and ^{3}CT states, facilitates the efficient RISC (or ISC) process, leading to high photoluminescence quantum yield (PLQY) for the ETC–TFDCNB complex. Further, we also extend the non-covalent approach to other donor–acceptor pairs to obtain various types of CT complexes, including TADF, exciplex, and fluorescent systems.[29]

In another instance, Zhang *et al.* synthesised two unique co-crystals consisting of, 2-(benzo[*d*]thiazol-2-yl)-3-(pyren-1-yl) acrylonitrile (Py-BZTCN) in *cis* and *trans* form as donor and TCNB as acceptor.[41] They discuss the formation of two polymorphic CT co-crystals, PCNTC-O (*cis*-Py-BZTCN : TCNB) and PCNTC-R (*trans*-Py-BZTCN : TCNB), with different photophysical properties based on the same donor (Py-BZTCN) and acceptor (TCNB) components (Fig. 7a). The different crystal packing and stoichiometric ratios between the donor and acceptor are induced by the *cis–trans* isomerism of the Py-BZTCN donor. The PCNTC-O co-crystal exhibits orange-yellow normal fluorescence, while the PCNTC-R co-crystal displays red thermally activated delayed fluorescence (TADF). The different photophysical behaviours are attributed to the formation of distinct CT complexes in the two co-crystals: a weak CT complex from pyrene to TCNB in PCNTC-O and a strong CT complex from Py to TCNB in PCNTC-R. Both co-crystals also demonstrate two-photon absorption properties.[43]

Recently, Barman *et al.* reported a series of twisted aromatic hydrocarbon (TAH) based CT co-crystals.[42] They demonstrated TADF-like enhanced luminescence, waveguide performance, and cellular imaging efficiency in the synthesised co-crystal. These findings support the development of cost-effective and scalable methods for efficient CT complex-based TADF emitters, potentially opening up new opportunities in optoelectronic device applications.[42] George and co-workers also used a similar

 This journal is © The Royal Society of Chemistry 2024

Published on 13 August 2024. Downloaded on 11/19/2024 1:41:25 PM.

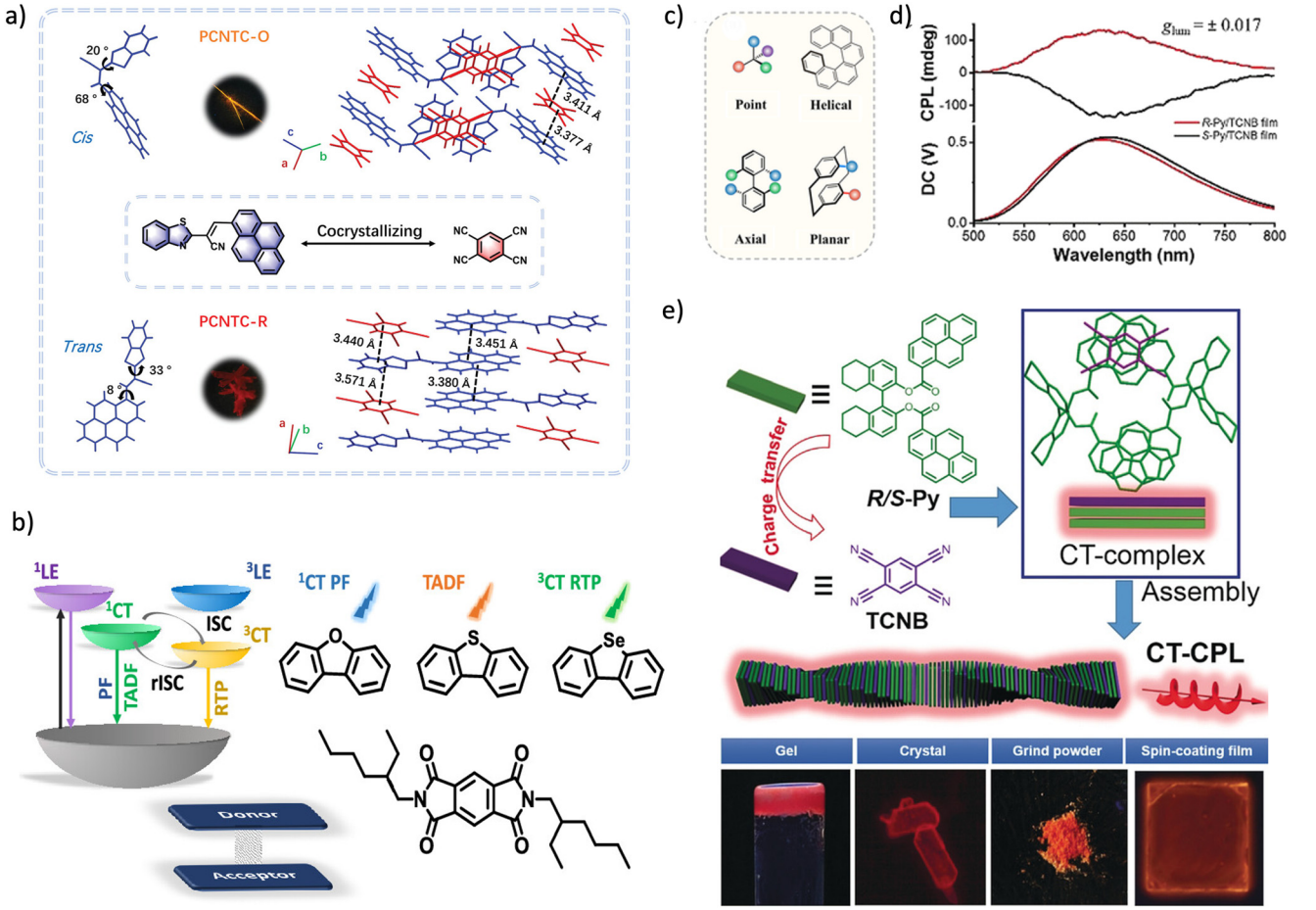

Fig. 7 a) Molecular structures of the Py-BZTCN and TCNB, crystal stacking, and photographs of PCNTC-O and PCNTC-R cocrystals (this figure has been adapted/reproduced from ref. 41 with permission from Wiley, copyright 2022); b) DBF, DBT, DBS and PmDI molecular structures, and a schematic Jablonski diagram of their OCTC (this figure has been adapted/reproduced from ref. 43 with permission from American Chemical Society, copyright 2023); c) types of chirality in molecular materials (this figure has been adapted/reproduced from ref. 47 with permission from Wiley, copyright 2021); d) CPL spectra of cast film of *R*/*S*-Py : TCNB CCTCs; e) chemical structures of the chiral donor (*R*/*S*-Py) and achiral acceptor TCNB. Schematic representation: CCTCs exhibiting strong CPL can be produced by combining chiral *R*/*S*-Py with the achiral TCNB. Fig. 7d and e has been adapted/reproduced from ref. 48 with permission from Wiley, copyright 2019.

modular, non-covalent donor–acceptor approach to tune the triplet harvesting pathways in arylene diimide-based phosphors.[43] The authors used pyromellitic diimide (PmDI) as an acceptor and combined it with different donors (dibenzofuran (DBF), dibenzothiophene (DBT), dibenzoselenophene (DBS)) to form 1 : 1 co-crystals. These co-crystals exhibited a wide range of emissions from singlet charge transfer (CT) fluorescence, thermally activated delayed fluorescence (TADF), and triplet CT phosphorescence, depending on the choice of the donor (Fig. 7b). Detailed photophysical studies revealed that the energy gap between the ^{1}CT and ^{3}CT states is crucial in determining the triplet harvesting pathway. The large energy gap in PmDI–DBF led to predominant fluorescence, while the small gap in PmDI–DBT resulted in TADF. Replacing sulfur with selenium in PmDI–DBS further stabilised the triplet state, leading to exclusive phosphorescence due to the heavy-atom effect. This kind of non-covalent approach provides an attractive strategy to control the triplet harvesting pathways in organic phosphors without tedious synthetic efforts, unlike conventional covalent donor–acceptor designs.[43]

6. CT complex-based approach to design circularly polarised luminescence (CPL) active material

Chiral charge transfer complexes (CCTCs) are a subset of CT complexes with supramolecular chirality.[47,48] Typically, a key focus in developing CPL-active materials revolves around achieving a high degree of luminescence dissymmetry, often denoted as g_{lum}. It's widely recognised that CT complexes have significant magnetic dipole transition moments and prevent electron dipole transition moments. As a result, there's growing interest in creating CPL active CT complexes with high g_{lum} value. This approach holds promise for advancing the development of CPL-active materials with substantial g_{lum} values, as described by the equation g_{lum} =

Published on 13 August 2024. Downloaded on 11/19/2024 1:41:25 PM.

$4|m|\cos\theta/|\mu|$, m and μ mean the magnetic and electric transition dipole moments, and θ is the angle between them. Thus, the organic CT complex with relatively large $|m|$ and depressed $|\mu|$ would produce better CPL with large g_{lum}. Chirality can be introduced in the CT pair by various means, such as using appropriate donor (or acceptor) units with a) point chirality, b) helical chirality, c) axial chirality, or d) planer chirality (Fig. 7c). Various fabrication methods, such as grinding, crystallisation, spin-coating, and gelatinisation, can create chiral emissive CT complexes by blending chiral donors and achiral acceptors.[47,48]

A seminal work by Han *et al.* focuses on achieving a large dissymmetry factor (g_{lum}) in circularly polarised luminescence (CPL) by utilising chiral charge-transfer (CT) complexes consisting of a chiral electron donor (*R*/*S*-Py) and an achiral electron acceptor (Fig. 7d and e). The chiral emissive CT complexes were formed by pairing a chiral electron donor (*R*/*S*-Py) (pyrene with axial chirality biphenyl group) with various achiral electron acceptors (*e.g.*, TCNB, TFQ, TCNE, TCNQ). In particular, *R*/*S*-Py:TCNB chiral emissive CT complexes exhibited CPL activity with a relatively large g_{lum} value of 0.017 (Fig. 7d). The structural synergy arising from π–π stacking and CT interactions enables the formation of supramolecular gels with enhanced CPL activity due to the large magnetic dipole transition moment in the CT state (Fig. 7e). Moreover, the authors have showed that CPL active chiral OCTC can be fabricated through various approaches, such as grinding, crystallization, spin coating, and gelation, by simply blending chiral donor (in particular *R*/*S*-Py) and achiral acceptor (TCNB). The study points towards the potential of these chiral emissive CT complexes in developing new strategies for designing highly efficient CPL-active materials, offering a novel approach to chiroptical functional materials with potential applications in multiple research fields.[48]

7. CT complex-based approach to design NIR emissive material

As outlined in the previous section, weak and moderate charge transfer complexes exhibit fascinating and distinct luminescent characteristics. Nevertheless, when a complex experiences intense charge transfer interactions, it often results in a non-luminescent state. This phenomenon occurs when the energy transferred during the charge transfer process is dissipated as heat rather than emitted as light. In luminescent complexes, such as those used in phosphorescence or fluorescence (prompt/delayed), the absorbed energy is typically re-emitted as light when electrons transition from excited to lower energy states. However, in complexes where strong charge transfer interactions dominate, the energy may be utilised in different ways, such as inducing structural changes or generating heat rather than emitting light. This section discusses the CT complex-based approach to get NIR or mid-IR emission utilising strong charge transfer interaction. Near-infrared (NIR) emissive organic materials are compounds that emit light in the near-infrared region of the electromagnetic spectrum. These materials have gained significant attention due to their potential applications in various fields, such as bioimaging, phototherapy, sensing, optical waveguides and optoelectronics.[49–53]

Developing efficient covalent NIR emissive materials often involves the tedious multistep chemical synthesis of conjugated organic molecules with specific molecular architectures that facilitate efficient light emission in the desired spectral range. In this context, the charge transfer complex-based approach is becoming promising as one can get solid-state NIR emissive material in a relatively simpler method. CT complexes can be engineered to emit light in the NIR region through various mechanisms, including molecular design, chemical modification, and careful optimisation of the electronic states(s) involved. Liao and co-workers recently reported a NIR-emissive CT complex, TP–F_4-TCNQ, with a maximum PL peak at 770 nm.[51] They used pyrene (Py) and triphenylene (TP) as essential electron donors and F_4TCNQ as an electron acceptor. In the resulting Py–F_4-TCNQ co-crystals, a distinctive mixed packing arrangement with robust π–π stacking was observed, contrasting with the segregated stacking mode found in TP–F_4TCNQ co-crystals (Fig. 8a). The differing counter pitch angles between the donors and acceptors, measuring 70° for Py–F_4TCNQ and 40° for TP–F_4TCNQ, significantly influenced the molecular packing modes. This modulation in packing geometry corresponded with varying degrees of charge transfer, as evidenced by CT degrees of 0.01850*e* for Py–F_4TCNQ and 0.00103*e* for TP–F_4TCNQ, indicating a comparatively stronger CT interaction in the former. Moreover, the enhanced electron spin resonance (ESR) intensity observed in Py–F_4-TCNQ co-crystals further underscored the robustness of the CT interaction in this system. The unique structural features of TP–F_4TCNQ co-crystals, characterised by a small counter-pitch angle and low CT degree, facilitated alterations in the forbiddance of CT-state electron transitions, ultimately enabling effective emission in the near-infrared (NIR) region beyond 760 nm (Fig. 8b), coupled with a notable photoluminescence quantum yield (PLQY) of 5.4%. The authors hypothesized that the TP–F_4TCNQ complex emits in the NIR region due to its segregated stack arrangement of TP and F_4TCNQ, whereas the mixed stack complex Py–F_4TCNQ is non-emissive. Moreover, TP–F_4TCNQ single-crystalline microwires demonstrate active optical waveguide properties in the NIR region.[51]

In a follow-up work, Liao and co-workers synthesised charge-transfer (CT) co-crystal through the self-assembly process using the electron donor dithieno[3,2-*b*:2′,3′-*d*] thiophene (DTT) and the standard receptor molecule 7,7,8,8-tetracyanoquinodimethane (TCNQ).[52] The highest occupied molecular orbital (HOMO) from the donor and the lowest unoccupied molecular orbital (LUMO) from the receptor resulted in a reduced overall energy gap for the CT co-crystal. This led to remarkable near-infrared (NIR) emission, peaking at 860 nm (Fig. 8c). Importantly, the biaxial electrostatic

 This journal is © The Royal Society of Chemistry 2024

Published on 13 August 2024. Downloaded on 11/19/2024 1:41:25 PM.

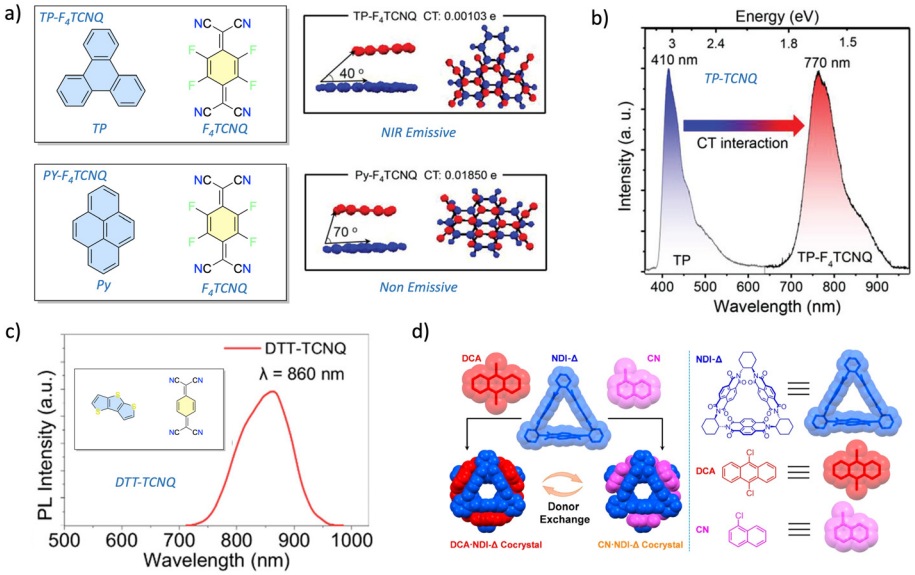

Fig. 8 a) Molecular structure of TP : F_4TCNQ and PY : F_4TCNQ complex. The counterpitch angles and the amount of CT are also shown. b) PL spectra of TP and TP–F_4TCNQ (Fig. 8a and b has been adapted/reproduced from ref. 51 with permission from Wiley, copyright 2022). c) The molecular structure of DTT and TCNQ (inset) and corresponding NIR emission of the DTT–TCNQ CT complex (this figure has been adapted/reproduced from ref. 52 with permission from American Chemical Society, copyright 2023). d) Structural formulas of NDI-Δ, DCA and CN: CT complex DCA·NDI-Δ and CN·NDI-Δ undergo reversible transformation based on the exchange of electron donors. The DCA·NDI-Δ co-crystal shows NIR emission (this figure has been adapted/reproduced from ref. 53 with permission from Springer Nature, copyright 2020).

interaction between the molecules facilitated a typical biaxial molecular packing mode in DTT–TCNQ CT complexes, as confirmed by high-resolution atomic force microscope images. The DTT–TCNQ composite shows a biaxial D–A packing mode, different from the typical directional D–A–D–A chain packing, which is an important reason for obtaining the desired NIR emission and sheet-like rectangular structure.[52]

In another instance, Stoddart and co-workers recently used the CT complex-based approach to realise a colour-tunable upconversion (close to NIR emission) based on the two co-crystals. They developed two charge transfer co-crystals, DCA·NDI-Δ and CN·NDI-Δ, composed of an electron-deficient naphthalenediimide-based triangular macrocycle (NDI-Δ) as the acceptor and different electron donors (9,10-dichloroanthracene (DCA) and 1-chloronaphthalene (CN)). The co-crystals exhibit distinctive optical properties, with DCA·NDI-Δ showing NIR emission and CN·NDI-Δ showing yellow emission. The DCA·NDI-Δ co-crystal exhibits more red-shifted absorption and emission compared to the CN·NDI-Δ co-crystal due to a difference in the degree of charge transfer (DCT). The porous DCA·NDI-Δ co-crystal can undergo reversible transformation to the CN·NDI-Δ co-crystal upon introduction of CN molecules and reformation of the DCA·NDI-Δ co-crystal upon removal of CN by solvent-vapor annealing. This transformation is accompanied by a change in the luminescence colour from red to yellow and back (Fig. 8d).[53] Overall, NIR emissive organic charge-transfer complex-based materials are promising for advancing various technological fields and addressing important challenges in healthcare, environmental monitoring, and energy conversion.

8. Integrating mechanical compliance in functional OCTCs

Integrating mechanical compliance, such as flexibility and/or self-healing properties, into functional OCTC crystals is a promising area of research that can enhance their practical applications and durability in optoelectronics, sensors, and other technologies. Crystal engineering becomes handy in designing and realising such an amalgamation of mechanical properties in functional OCTCs. Some empirical ideas to achieve such a complex symphony include: a) choosing donor and acceptor molecules with inherent flexibility. This can be achieved by incorporating flexible linkers (*e.g.*, alkyl chains, ether linkages) chains into the molecular structure of the coformers. b) Utilise hydrogen bonding and/or van der Waals interactions to create flexible supramolecular networks. c) Introduce dynamic covalent bonds or reversible non-covalent interactions that can break and reform, allowing the material to heal itself. These interactions can help dissipate stress and contribute to flexibility and/or self-healing.[40,54–56] Pioneering works by Reddy and co-workers are milestones in designing flexible and self-healing organic crystals.[57–59] The detailed mechanism of mechanically compliant organic crystals is beyond the scope of discussion of this highlight and can be found elsewhere.[57–59] Although mechanically adaptive molecular crystals have garnered significant interest due to their unique properties and potential applications in various fields, there are only a handful of reports of such compliance in functional OCTCs.[60,61] Some of the mechanically compliant OCTCs are highlighted from here

Published on 13 August 2024. Downloaded on 11/19/2024 1:41:25 PM.

onwards. Chopra *et al.* have reported an elastic OCTC crystal DQP3 (1A : 2 × 0.5D), which contained two half molecules of pyrene (donor) and one molecule of 1,8-dinitroanthraquinone (acceptor) in the asymmetric unit.[60a] Between 2.50 and 2.78 Å, the donor and acceptor molecules are connected by C–H···O hydrogen-bonding interactions. They then piled into interlocked columns parallel to the *ac* plane along the *a*-axis, preventing slip planes from forming between the columns. As a result, under mechanical external force, the acicular co-crystal, DQP3 (1A : 2 × 0.5D), demonstrated elastic bending with a bending angle that almost exceeded 180°.[60a] A novel OCTC co-crystal solvate was created by slowly evaporating a tetrahydrofuran (THF) solution containing perylene and 1,2,4,5-tetracyanobenzene in a 1 : 1 ratio in Hu's group.[61] The molecules of planar donor (perylene) and acceptor (1,2,4,5-tetracyanobenzene) formed a stacked sequence along the *c*-axis. The solvated CT co-crystal emitted red light with a photoluminescence quantum yield of 5.04% and had a fluorescence decay lifetime of 9.68 ns. However, when exposed to air, it gradually turned greyish-green due to the loss of THF molecules. Upon exposure to THF vapour, the solvent-free CT co-crystal regained its red colour and exhibited significant mechanical bending. This reversible THF absorption and desorption process induced continuous mechanical bending and colour changes. Additionally, similar solvatomechanical behaviour and colour changes were observed with other solvents like 1,4-dioxane, providing a promising platform for studying mechanical motions in solvent-responsive CT co-crystals.[61] However, mechanically compliant OCTCs with the aforementioned optical properties (phosphorescent, TADF, NIR emission) are minuscule in the literature.[40] There is a lot of room to work in that direction. Thus, integrating mechanical compliance into functional OCTC crystals involves a multi-faceted approach that includes material design, crystal engineering, characterisation, and theoretical modelling. By carefully selecting and modifying the donor and acceptor molecules and optimising the crystal packing, it is possible to develop flexible and self-healing OCTC crystals with robust optoelectronic properties. This integration opens up new avenues for advanced applications in flexible electronics, wearable devices, and more.

The above discussion on OCTCs represents the tip of the iceberg regarding their potential applications. Characterised by their unique electronic properties, these complexes hold promise in various cutting-edge technologies. For instance, they are pivotal in developing organic photovoltaics, where their efficient charge separation and transport properties can significantly enhance solar cell performance. Additionally, OCTCs are being explored in organic field-effect transistors (OFETs) and light-emitting diodes (OLEDs) for flexible and wearable electronics.[5–7,62] Their tunable electronic interactions also make them suitable for use in sensors and bioelectronics, paving the way for advancements in medical diagnostics and environmental monitoring. The vast potential of OCTCs is only beginning to be uncovered, hinting at a future prosperous with innovation and discovery.

Data availability

No original data is provided in the manuscript.

Conflicts of interest

The authors declare no conflict of interest.

References

1 L. B. Coleman, M. J. Cohen, D. J. Sandman, F. G. Yamagishi, A. F. Garito and A. J. Heeger, *Solid State Commun.*, 1973, **12**, 1125–1132.
2 J. Ferraris, D. O. Cowan, V. Walatka and J. H. Perlstein, *J. Am. Chem. Soc.*, 1973, **95**, 948–949.
3 J. Zhang, W. Xu, P. Sheng, G. Zhao and D. Zhu, *Acc. Chem. Res.*, 2017, **50**, 1654–1662.
4 A. A. Dar and S. Rashid, *CrystEngComm*, 2021, **23**, 8007–8026.
5 (*a*) J. Guo, Y. Zeng, Y. Zhen, H. Geng, Z. Wang, Y. Yi, H. Dong and W. Hu, *Angew. Chem., Int. Ed.*, 2022, **61**, e202202336; (*b*) M. A. Niyas, R. Ramakrishnan, V. Vijay and M. Hariharan, *Chem. – Eur. J.*, 2018, **24**, 12318–12329.
6 K. P. Goetz, D. Vermeulen, M. E. Payne, C. Kloc, L. E. McNeil and O. D. Jurchescu, *J. Mater. Chem. C*, 2014, **2**, 3065–3076.
7 L. Sun, Y. Wang, F. Yang, X. Zhang and W. Hu, *Adv. Mater.*, 2019, **31**, 1902328.
8 R. Bhowal, S. Biswas, D. P. Adiyeri Saseendran, A. L. Koner and D. Chopra, *CrystEngComm*, 2019, **21**, 1940–1947.
9 W. Wang, L. Luo, P. Sheng, J. Zhang and Q. Zhang, *Chem. – Eur. J.*, 2021, **27**, 464–490.
10 X. Ye, Y. Liu, Q. Guo, Q. Han, C. Ge, S. Cui, L. Zhang and X. Tao, *Nat. Commun.*, 2019, **10**, 761.
11 (*a*) L. S. Germann, M. Arhangelskis, M. Etter, R. E. Dinnebier and T. Friščić, *Chem. Sci.*, 2020, **11**, 10092–10100; (*b*) Y. Xiao, C. Wu, X. Hu, K. Chen, L. Qi, P. Cui, L. Zhou and Q. Yin, *Cryst. Growth Des.*, 2023, **23**, 4680–4700.
12 S. N. Madanayake, A. Manipura, R. Thakuria and N. M. Adassooriya, *Org. Process Res. Dev.*, 2023, **27**, 409–422.
13 N. M. Adassooriya, S. P. Mahanta and R. Thakuria, *CrystEngComm*, 2022, **24**, 1679–1689.
14 D. Hasa, G. S. Rauber, D. Voinovich and W. Jones, *Angew. Chem., Int. Ed.*, 2015, **54**, 7371–7375.
15 S. K. Park, J. H. Kim, T. Ohto, R. Yamada, A. O. F. Jones, D. R. Whang, I. Cho, S. Oh, S. H. Hong, J. E. Kwon, J. H. Kim, Y. Olivier, R. Fischer, R. Resel, J. Gierschner, H. Tada and S. Y. Park, *Adv. Mater.*, 2017, **29**, 1701346.
16 M. Wykes, S. K. Park, S. Bhattacharyya, S. Varghese, J. E. Kwon, D. R. Whang, I. Cho, R. Wannemacher, L. Lüer, S. Y. Park and J. Gierschner, *J. Phys. Chem. Lett.*, 2015, **6**, 3682–3687.
17 A. Mandal and B. Nath, *CrystEngComm*, 2022, **24**, 6669–6676.
18 Y. Huang, Z. Wang, Z. Chen and Q. Zhang, *Angew. Chem., Int. Ed.*, 2019, **58**, 9696–9711.

 This journal is © The Royal Society of Chemistry 2024

Published on 13 August 2024. Downloaded on 11/19/2024 1:41:25 PM.

19 A. A. Kongasseri, S. N. Ansari, S. Garain, S. M. Wagalgave and S. J. George, *Chem. Sci.*, 2023, **14**, 12548–12553.
20 S. K. Park, S. Varghese, J. H. Kim, S.-J. Yoon, O. K. Kwon, B.-K. An, J. Gierschner and S. Y. Park, *J. Am. Chem. Soc.*, 2013, **135**, 4757–4764.
21 R. Kumar, H. Aggarwal, R. Bhowal, D. Chopra and A. Srivastava, *Chem. – Eur. J.*, 2019, **25**, 10756–10762.
22 D. Sharada, A. Saha and B. K. Saha, *New J. Chem.*, 2019, **43**, 7562–7566.
23 A. Khan, R. Usman, S. M. Sayed, R. Li, H. Chen and N. He, *Cryst. Growth Des.*, 2019, **19**, 2772–2778.
24 H. Jiang, P. Hu, J. Ye, K. K. Zhang, Y. Long, W. Hu and C. Kloc, *J. Mater. Chem. C*, 2018, **6**, 1884–1902.
25 (*a*) D. N. Sathyanarayana, *Electronic Absorption Spectroscopy and Related Techniques*, Universities Press, 2001; (*b*) *Organic Electronics: Materials, Processing, Devices and Applications*, ed. F. So, CRC Press, 2009.
26 R. Thakuria, N. K. Nath and B. K. Saha, *Cryst. Growth Des.*, 2019, **19**, 523–528.
27 S. Biswas and A. Das, *ChemNanoMat*, 2021, **7**, 748–772.
28 J.-C. Christopherson, F. Topić, C. J. Barrett and T. Friščić, *Cryst. Growth Des.*, 2018, **18**, 1245–1259.
29 K. J. Kalita, S. Mondal, C. M. Reddy and R. K. Vijayaraghavan, *Chem. Sci.*, 2023, **14**, 13870–13878.
30 (*a*) M. Singh, K. Liu, S. Qu, H. Ma, H. Shi, Z. An and W. Huang, *Adv. Opt. Mater.*, 2021, **9**, 2002197; (*b*) H. Zheng, Z. Zhang, S. Cai, Z. An and W. Huang, *Adv. Mater.*, 2024, **36**, 2311922.
31 M. Singh, K. Shen, W. Ye, Y. Gao, A. Lv, K. Liu, H. Ma, Z. Meng, H. Shi and Z. An, *Angew. Chem., Int. Ed.*, 2024, **63**, e202319694.
32 V. Gude and K. Biradha, *J. Phys. Chem. C*, 2021, **125**, 120–129.
33 S. Garain, S. N. Ansari, A. A. Kongasseri, B. Chandra Garain, S. K. Pati and S. J. George, *Chem. Sci.*, 2022, **13**, 10011–10019.
34 J. Vainauskas, T. H. Borchers, M. Arhangelskis, L. J. McCormick McPherson, T. S. Spilfogel, E. Hamzehpoor, F. Topić, S. J. Coles, D. F. Perepichka, C. J. Barrett and T. Friščić, *Chem. Sci.*, 2023, **14**, 13031–13041.
35 Y. Wen, S. Zhao, Z. Yang, Z. Feng, Z. Yang, S.-T. Zhang, H. Liu and B. Yang, *J. Phys. Chem. Lett.*, 2024, **15**, 2690–2696.
36 K. Liu, S. Li, L. Fu, Y. Lei, Q. Liao and H. Fu, *Nanoscale*, 2022, **14**, 6305–6311.
37 A. Abe, K. Goushi, M. Mamada and C. Adachi, *Adv. Mater.*, 2024, **36**, 2211160.
38 T. Zhu, S. Zheng, T. Yang and W. Z. Yuan, *J. Phys. Chem. Lett.*, 2023, **14**, 6451–6458.
39 (*a*) M. Y. Wong and E. Zysman-Colman, *Adv. Mater.*, 2017, **29**, 1605444; (*b*) Q. Xue and G. Xie, *Adv. Opt. Mater.*, 2021, **9**, 2002204.
40 L. Sun, W. Hua, Y. Liu, G. Tian, M. Chen, M. Chen, F. Yang, S. Wang, X. Zhang, Y. Luo and W. Hu, *Angew. Chem., Int. Ed.*, 2019, **58**, 11311–11316.
41 X. Zhang, J. De, H. Liu, Q. Liao, S.-T. Zhang, C. Zhou, H. Fu and B. Yang, *Adv. Opt. Mater.*, 2022, **10**, 2200286.
42 D. Barman, M. Annadhasan, A. P. Bidkar, P. Rajamalli, D. Barman, S. S. Ghosh, R. Chandrasekar and P. K. Iyer, *Nat. Commun.*, 2023, **14**, 6648.
43 A. A. Kongasseri, S. Garain, S. N. Ansari, B. C. Garain, S. M. Wagalgave, U. Singh, S. K. Pati and S. J. George, *Chem. Mater.*, 2023, **35**, 7781–7788.
44 S. K. Lower and M. A. El-Sayed, *Chem. Rev.*, 1966, **66**, 199–241.
45 A. L. Schleper, K. Goushi, C. Bannwarth, B. Haehnle, P. J. Welscher, C. Adachi and A. J. C. Kuehne, *Nat. Commun.*, 2021, **12**, 6179.
46 F. B. Dias, J. Santos, D. R. Graves, P. Data, R. S. Nobuyasu, M. A. Fox, A. S. Batsanov, T. Palmeira, M. N. Berberan-Santos, M. R. Bryce and A. P. Monkman, *Adv. Sci.*, 2016, **3**, 1600080.
47 X. Li, Y. Xie and Z. Li, *Adv. Photonics Res.*, 2021, **2**, 2000136.
48 J. Han, D. Yang, X. Jin, Y. Jiang, M. Liu and P. Duan, *Angew. Chem., Int. Ed.*, 2019, **58**, 7013–7019.
49 M.-P. Zhuo, X.-D. Wang and L.-S. Liao, *Small Sci.*, 2022, **2**, 2200029.
50 L. An, L. Zheng, C. Xu, Z. Zhao, F. Gao, W. Wang, C. Ou and X. Dong, *Small Struct.*, 2023, **4**, 2200220.
51 M.-P. Zhuo, Y. Yuan, Y. Su, S. Chen, Y.-T. Chen, Z.-Q. Feng, Y.-K. Qu, M.-D. Li, Y. Li, B.-W. Hu, X.-D. Wang and L.-S. Liao, *Adv. Mater.*, 2022, **34**, 2107169.
52 C.-F. Xu, Y.-P. Liu, Y. Yu, X.-Y. Meng, H. Zong, Q. Lv, X.-Y. Xia, X.-D. Wang and L.-S. Liao, *J. Phys. Chem. Lett.*, 2023, **14**, 3047–3056.
53 Y. Wang, H. Wu, P. Li, S. Chen, L. O. Jones, M. A. Mosquera, L. Zhang, K. Cai, H. Chen, X.-Y. Chen, C. L. Stern, M. R. Wasielewski, M. A. Ratner, G. C. Schatz and J. F. Stoddart, *Nat. Commun.*, 2020, **11**, 4633.
54 K. J. Kalita, S. Mondal, C. M. Reddy and R. K. Vijayaraghavan, *Chem. Mater.*, 2023, **35**, 709–718.
55 P. Deka, S. Das, P. Sarma, K. J. Kalita, R. K. Vijayaraghavan, C. M. Reddy and R. Thakuria, *Cryst. Growth Des.*, 2024, **24**, 2322–2330.
56 P. Gupta, D. P. Karothu, E. Ahmed, P. Naumov and N. K. Nath, *Angew. Chem., Int. Ed.*, 2018, **57**, 8498–8502.
57 S. Saha, M. K. Mishra, C. M. Reddy and G. R. Desiraju, *Acc. Chem. Res.*, 2018, **51**, 2957–2967.
58 S. Mondal, P. Tanari, S. Roy, S. Bhunia, R. Chsowdhury, A. K. Pal, A. Datta, B. Pal and C. M. Reddy, *Nat. Commun.*, 2023, **14**, 6589.
59 S. Bhunia, S. Chandel, S. K. Karan, S. Dey, A. Tiwari, S. Das, N. Kumar, R. Chowdhury, S. Mondal, I. Ghosh, A. Mondal, B. B. Khatua, N. Ghosh and C. M. Reddy, *Science*, 2021, **373**, 321–327.
60 (*a*) M. Singh and D. Chopra, *Cryst. Growth Des.*, 2018, **18**, 6670–6680; (*b*) M. Ghora, R. K. Manna, S. K. Park, S. Oh, S.-I. Kim, S. Y. Park, J. Gierschner and S. Varghese, *Chem. – Eur. J.*, 2024, e202401023.
61 Y. Sun, Y. Lei, H. Dong, Y. Zhen and W. Hu, *J. Am. Chem. Soc.*, 2018, **140**, 6186–6189.
62 F. Zhang, X. Dai, W. Zhu, H. Chung and Y. Diao, *Adv. Mater.*, 2017, **29**, 1700411.